Long term measurements of neutron dose rates at Testa Grigia high altitude research station (3480 m. a.s.l.)

S. Vernetto [a,b,*], M. Laurenza [c], M. Storini [c], A. Zanini [b], P. Diego [c], S. Massetti [c], A. Liberatore [a], J. C. Terrazas [d], C. Vigorito [b,e], P. Vallania [a,b], S. Cirilli [f,g]

[a] INAF-OATO, Via Pietro Giuria 1, 10125 Torino, Italy
[b] INFN Sezione Torino, Via Pietro Giuria 1, 10125 Torino, Italy
[c] INAF-IAPS, Via del Fosso del Cavaliere 100, 00133 Roma, Italy
[d] Departamento de Física, Universidad Mayor de San Simón, Cochabamba, Bolivia
[e] Dipartimento di Fisica, Università degli Studi di Torino, via P.Giuria 1, 10125, Torino, Italy
[f] Dipartimento di Matematica e Geoscienze, Università degli Studi di Trieste, via Valerio 2, 34127, Trieste, Italy
[g] INFN Sezione Trieste, via Valerio 2, 34127, Trieste, Italy

A B S T R A C T

At the Testa Grigia high altitude research Station (3480 m. a.s.l, Italy, 45°57′ N, 7°42' E) several dosimetric campaigns for the measurement of the dose due to secondary neutrons produced in the atmosphere and in the surrounding environment by primary cosmic rays have been carried out from 2014 until 2021. Because of the high altitude of the site, the neutron flux at Testa Grigia is 10–15 times higher than at the sea level. Various instruments has been used to evaluate the dependence of the ambient dose equivalent rate from different factors as atmospheric parameters, environmental conditions and solar activity. Moreover, since October 2014 a modular neutron monitor designed, realized and tested by the SVIRCO Observatory Group INAF-IAPS in Rome, is permanently operating in the laboratory, providing a continuous monitoring of primary cosmic ray variability and making the laboratory an ideal place for dosimetric studies, instrument calibration and "in field" tests. In this paper the results of several neutron measurements carried out in the last years in periods of different solar activity and environmental conditions are reported, with a discussion on the origin of the observed variations of the ambient dose equivalent rate.

1. Introduction

The Testa Grigia Laboratory (Italy, 45.95° N, 7.7° E, vertical rigidity cutoff $R_V = 4.71$ GV in 2015), located on the Italy-Switzerland boundary at an altitude of 3480 m a.s.l. at the edge of the Plateau Rosa Glacier, was built in 1947 for pioneering measurements on cosmic rays. Since then it has been used for researches on different topics: astrophysics, dosimetry, atmospheric physics, high altitude medical studies. Presently it is owned by the Italian National Research Council (CNR).

At high mountain altitude, the neutron contribution to the total dose become significant because of the reduced atmospheric absorption layer and the study of its temporal variations related to the solar activity or other phenomena is of great interest. At the altitude of the laboratory (the second highest in Europe), the neutron flux is 10–15 times higher than at the sea level, making the Testa Grigia a suitable site for dosimetric studies and instruments calibration. A historical series of

neutrons dosimetric data has been collected in the last two and half decades [Manfredotti et al., 1997; Zanini et al., 2001, 2005, 2009]. In the last years, measurements of the neutron ambient dose equivalent have been regularly performed by the INFN Turin group. Moreover, in October 2014 it has been installed a modular neutron monitor, realized by the group at INAF-IAPS handling the SVIRCO (acronym for study of cosmic ray variations) Observatory, i.e. the Rome neutron monitor [Signoretti et al., 2013]. Since then the instrument is in stable operation in the laboratory, providing a continuous monitoring of the primary cosmic ray variability. The simultaneous measurements of the neutron ambient dose equivalent with dedicated instrumentation as well as the monitoring of cosmic ray intensity with the neutron monitor is relevant for the analysis of the different sources of dose variations.

Neutrons detected at ground level are mostly secondary neutrons produced in atmosphere by the hadronic component of air showers induced by Galactic cosmic rays interacting with nitrogen and oxygen

---

* Corresponding author. INAF-OATO, Via Pietro Giuria 1, 10125 Torino, Italy.

nuclei. The neutron spectrum is the combination of different components: *cascade* neutrons, with energies ranging from ~20 MeV to several GeVs, *evaporation* neutrons emitted by excited nuclei, with typical energies around a few MeVs, *thermal* and *epithermal* neutrons produced in the moderation processes in atmosphere and in the ground. While the flux of neutrons of energy above ~20 MeV is mainly directed downwards, the flux of thermal and epithermal neutrons is distributed in the whole solid angle, with a significant fraction coming from interactions in the ground (albedo neutrons), whose intensity depends on the soil composition and on the spatial distribution of ground, rocks, water, buildings located in the surroundings, up to distances of tens or hundreds meters. The differential spectrum multiplied by the energy has three evident peaks: the thermal peak at ~0.025 eV, the evaporation peak at a few MeV and the cascade peak at ~100 MeV. The first measurements of the neutron spectrum date back to the late 1950's [Hess et al., 1959]. Since then, measurements of neutron spectra have been performed in several locations, with variable fluxes depending on latitude, altitude and environment conditions (see for example Zanini et al., 2001, Nakamura et al., 2005; Kowatari et al., 2005; Vega-Carrillo and Manzanares-Acuna, 2004; Rühm et al., 2009; Cheminet et al., 2014, Hubert et al., 2016).

Considering the spectrum shape and the dependence of the dose on the neutron energy (see discussion in Section 3.2), most of the dose is due to evaporation and cascade neutrons, that contribute to the dose with comparable amounts. The dose due to neutrons with energy less than 100 keV is a few percent of the total.

The temporal variations of the neutron flux and dose rate, are mainly due to:

a) Solar activity. Cosmic rays that mostly contribute to the neutron flux at ground have energies below a few tens of GeV and are modulated by the solar activity, producing corresponding variations of the neutron flux, whose amplitude depends on the geomagnetic rigidity cutoff. Moreover, the rotation of the Earth inside the non-uniform interplanetary magnetic field also produces a local modulation of the cosmic ray flux with a 24 h solar time period, that produces counting rate variations in neutron monitors of amplitude of order 1% [Moraal et al., 2000].

b) Changes in atmospheric pressure, that modifying the target thickness, affects the secondary particle flux. An increase of 1 hPa of the air pressure produces a decrease of about 0.7% of the cascade neutron flux [Bütikofer, 2018].

c) Environmental conditions. The presence of water/snow in the atmosphere and in the soil produces significant effects on neutrons since the hydrogen is a very efficient moderator. The flux of neutrons of energy above ~20 MeV is weakly dependent on the water/snow on the ground and in the air, but can be moderated/absorbed by snow accumulation on the building hosting the detector. On the contrary, the flux at lower energies contains a significant fraction of albedo neutrons coming from downwards and horizontal directions, whose intensity is affected by the presence of water/snow in the soil up to significant distances from the detector [Hubert et al., 2016].

In the following we report the results of some measurements carried out in the last years with several neutron detectors, operating in different energy range, under different levels of solar activity and environmental conditions. The simultaneous measurements performed by different instruments is of particular interest since it allows to disentangle the effects of dose variations due to phenomena of different origin.

2. Materials and methods

The data presented in this work have been collected with the following instruments:

a) Modular Neutron Monitor
b) Rem counter Atomtex BDKN-03
c) Rem counter Thermo Wendi-2
d) Rem counter KWD Digipig (NM2222A He-3)
e) Liulin-AR Silicon spectrometer
a) Modular Neutron Monitor

The modular neutron monitor installed at the Testa Grigia laboratory (referred from now on as TG-NM) was designed, realized and tested at the SVIRCO Observatory in Rome [Signoretti et al., 2013]. The general design of the TG-NM has a variable geometry to be adapted to counters of different lengths [Signoretti and Storini, 2011]. In the Testa Grigia configuration, it consists of a LND 25373 ^{3}He proportional counter [LND, INC. website] of length 190.8 cm and diameter 5.08 cm, surrounded by 23 modules, each composed by a polyethylene reflector, with a hole housing a lead ring (producer) and a polyethylene inner moderator (Fig. 1). Each component is reasonably light, since the weight of the heaviest element is lower than 23 Kg, so only one operator is required for transporting and assembling the whole neutron monitor even in its biggest arrangement (about 800 kg). The possibility to transport it easily makes the instrument suitable for measurements in high mountains sites or in remote locations that are difficult to access.

Before the installation at the TG laboratory, the modular neutron monitor was tested against the standard 20NM-64 neutron monitor in Rome (composed of 20 counters) during the period 1 April – July 13, 2010 [Signoretti and Storini, 2011]. The estimated intensity reference level was 146 counts min^{-1} vs 9372 counts min^{-1} for the former and the latter, respectively. Thus, the modular detector has a lower counting rate which is approximately 1.5% of the 20NM-64 (roughly corresponding to 31% of a single detector of a standard NM). After installation, its performance has been checked by comparing its data with those of the Jungfraujoch neutron monitors [Flückiger and Bütikofer, 2009] operating at comparable altitude and rigidity cutoff. Fig. 2 reports the TG-NM pressure corrected percent variations on 2 h basis computed with respect to the mean value over 20 days in summer 2016, compared with the corresponding data of the 18-IGY Neutron Monitor at the Jungfraujoch (JF) Sphinx Observatory [Jungfraujoch NM data website], located in Switzerland at m a.s.l. (46.55°N, 7.98°E, vertical rigidity cutoff $V_R = 4.54$ GV in 2015). In this time interval the TG-NM average counting rate was 1730 min^{-1}. The root mean square deviation of the differences between the two data sets is 0.38%.

b) Rem counter Atomtex BDKN-03

This neutron detector is a ^{3}He proportional counter with a polyethylene moderator. It works in the energy range 0.025 eV < E_n < 14 MeV and can measure dose rates (in term of ambient dose equivalent H* (10)) ranging from 0.1 μSv/h to 10 mSv/h, with an intrinsic measurement error of 20%. Due to its energy range, this instrument detects thermal and evaporation neutrons, being much less sensitive to cascade neutrons.

c) Rem Counter THERMO WENDI-2

This detector consists of a ^{3}He counter in a polyethylene moderator with included a tungsten powder shell. High energy neutrons cause spallation reactions in the tungsten nuclei producing further neutrons of lower energies. In this way the sensitivity is extended to energies up to 5 GeV and cascade neutrons can be detected. Wendi-2 can measure dose rates from 0.001 μSv/h to 100 mSv/h. Together with the BDKN-03, it has been tested at the TG Laboratory in 2014 and 2017 before being used in two dosimetric campaigns (CORA and HALCORD) at the Antarctica base of Marambio.
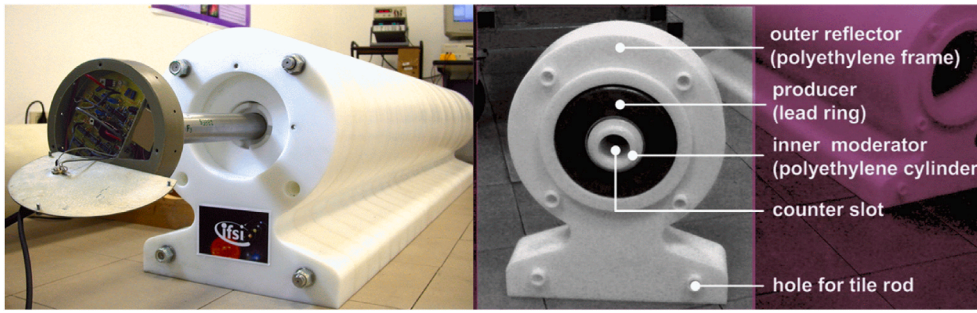
d) Rem counter KWD Digipig (NM2222A He-3)

Fig. 1. Modular neutron monitor used at the Testa Grigia Laboratory. The whole structure of the detector, which is composed by 23 adjacent modules, is closed by a plate at both ends. The frontal plate has a hole for the counter and a bay for the electronics head. On the right panel, a single module is shown.
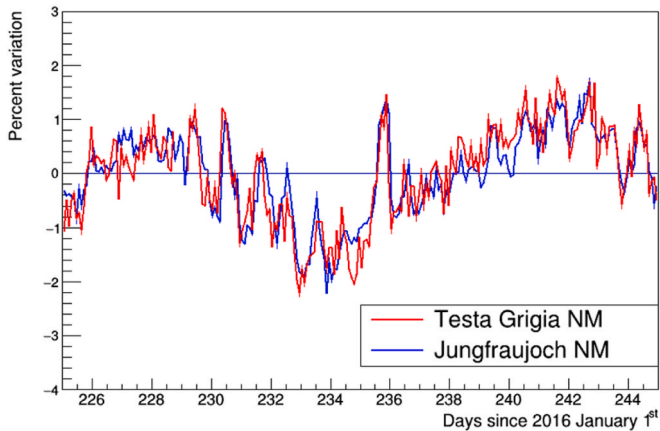

Fig. 2. Percent variations (2 h average) of Testa Grigia NM and 18-IGY Jungfraujoch NM counting rates during 20 days from 13 August to September 1, 2016.

This instrument consists of a ^{3}He counter with polyethylene and boron plastic as moderators. The nominal energy range is 0.025 eV $< E_n < 17$ MeV. As the BDKN-03, it mainly detects thermal to evaporation neutrons. It can measure dose rates from 0.001 mSv/h to 1 Sv/h.

e) Liulin-AR Silicon Spectrometer

The Liulin LET spectrometer, developed and produced at the Solar-Terrestrial Influence Laboratory of Bulgarian Academy of Sciences in Sofia, is based on a 256-channels active silicon semiconductor detector [Dachev, 2009]. The instrument is able to monitor the energy deposition spectra, fluxes and doses in mixed radiation fields. An HAMAMATSU S2744-08 PIN diode with an effective area of 10×20 mm^2 and thickness 300 μm is the sensitive volume. The deposited energy is measured in the energy range from 81.3 keV to 20.8 MeV, corresponding to a LET (Linear Energy Transfer) deposition in silicon in the range 0.135–69.4 keV/μm. Liulin type spectrometers are custom made for specific applications. The Liulin-I MDU-01 was used in several dosimetric campaigns in Antarctica and South America from 2013 to 2020 [Zanini et al., 2019]. The Liulin-AR considered here has been specifically developed to be installed aboard the Argentine-Brasilian SABIA-MAR satellite, to be launched in 2023. It has also been used in 2017 to collect data for 10 days at the Italy-French base Concordia in Antarctica [Zanini et al., 2019].

3. Results and discussions

3.1. Neutron monitor data

The Neutron Monitor operating at the Testa Grigia Laboratory has been recording data since November 2014, covering the descending phase of the 24th solar cycle, with two periods of non-operation in 2017 and 2018. Secondary neutrons that mostly contribute to neutron monitors counting rate are those of energy from ~100 MeV to a few GeV, i.e. those referred as cascade neutrons [Clem and Dorman, 2000].

Besides primary cosmic ray intensity modulations due to solar activity, the main sources of neutron monitor counting rate variations are changes in atmospheric pressure, which affect the secondary neutron flux up to 20–25% at Testa Grigia. The TG-NM counting rates are corrected for pressure variation to the reference pressure of 642.6 hPa using a barometric coefficient of 0.72% hPa^{-1}, the same values adopted by the Jungfraujoch neutron monitors, that have a similar altitude and rigidity cutoff [Jungfraujoch NM data website].

A local source of counting rate variations is the snow that in winter time accumulates on the roof and against the walls of the laboratory. At the Testa Grigia the snowfall is significant during several months, and due to the strong winds, the snowpack on the roof and outside the laboratory is irregularly distributed. The snow is not removed for the whole winter season.

Fig. 3 shows the percent variation of TG-NM counting rate (corrected for the atmospheric pressure) from 2014 to 2020, compared with the data of the 18-IGY Neutron Monitor at the Jungfraujoch Sphinx Observatory (referred from now on as TG-JF). A significant decrease (17% at most) of the counting rate of TG-NM with respect to that of JF-NM is visible in winter and particularly in spring time, due to the snow effect. In June–July the snow melts and the counting rate recovers completely, returning to the level of JF-NM (where the snow is removed after every snowfall) within a difference of less than 1%.

Besides the depression due to the snow, variations of the TG-NM counting rate on time scales of several days are also visible and are strongly correlated with JF-NM data. Such variations are due to the effect of interplanetary perturbations, e.g., high speed streams which are dominant during the decreasing and minimum phases of solar activity. On time scales of years, the counting rate shows a slow and regular increase by about 10% from 2014 to 2020, due to the decreasing solar activity, that reached the minimum at the end of 24th solar cycle in 2019.

According to [Zweck et al., 2013], high energy neutrons in snow are moderated and absorbed, resulting in an exponential decrease of the flux with a mean free path of $\lambda_{snow} = 109$ g cm^{-2}. Assumed that the observed decrease is due to the snow, we calculated the effective snow thickness d_{swe} (in unit of water equivalent) from the expression R/R$_0$ = 1- exp (-d_{swe}/λ_{snow}), where R is the measured rate and R$_0$ the "corrected rate", obtained by increasing the TG-NM counting rate to a level consistent with JF-NM data. Obviously this procedure assumes that JF-NM is not affected by the snow (an assumption that is valid most of the time, but probably some snow accumulation is present before snow removals).

Fig. 4 reports the obtained daily values of d_{swe} as a function of time. The thickness d_{swe} does not represent the real snow thickness on the roof, but rather the average effect of irregular snow accumulations due to the wind. It has to be noted that in the '90s a metal platform with a large box structure has been built over the Testa Grigia laboratory to host instruments for atmospheric studies, and inside this box the snow
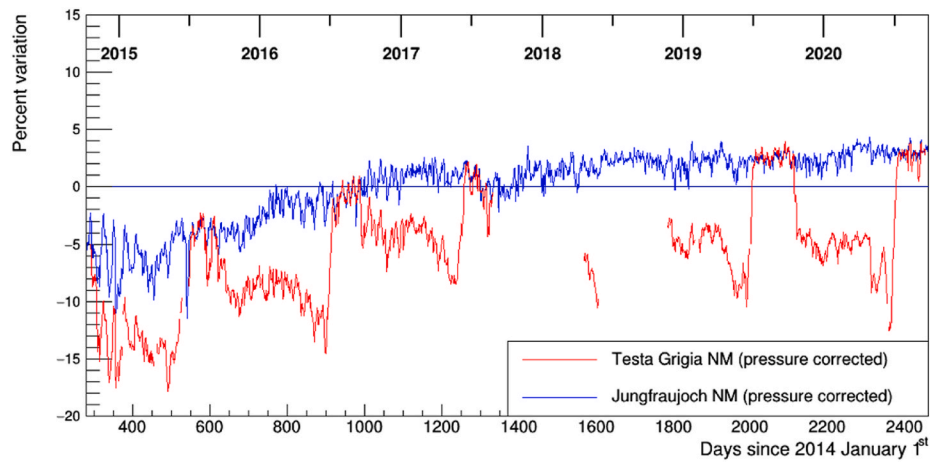
Fig. 3. Daily percent variation of the Testa Grigia and Jungfraujoch 18-IGY neutron monitors counting rates, with respect to the average counting rate of day 956 (August 13, 2016). In winter time the TG-NM counting rate is affected by the neutron absorption by the snow on the laboratory roof.
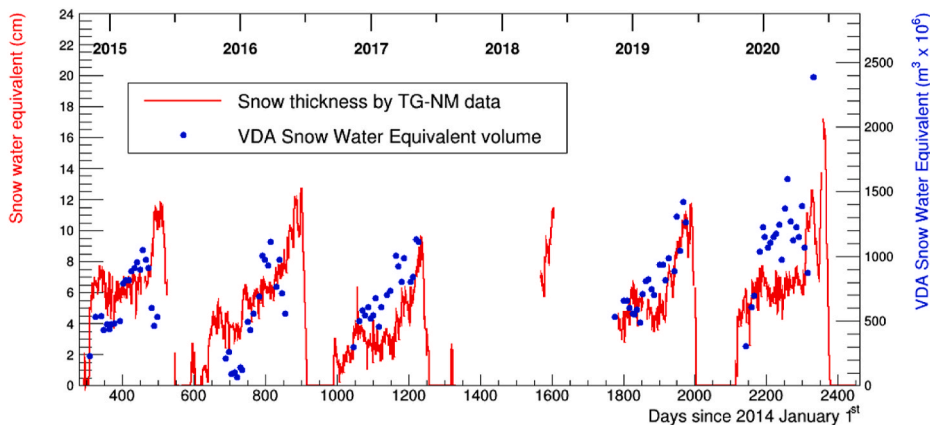

Fig. 4. Red line: snow water equivalent thickness corresponding to the decrease of the Testa Grigia neutron monitor counting rate (scale on the left). The blue points represent the Snow Water Equivalent volume (SWE) in the whole region of the Aosta Valley (VDA) evaluated by the Regional Environmental Protection Agency (ARPA) (scale on the right).

accumulates in irregular ways. Isolated peaks in Fig. 4, as for example the one around day 590 corresponds to a few days of snowfall in August 2015, according to meteorological data [Meteomanz website]. It is interesting the steep increase visible every year in May–June just before the melting time, probably due to some resistant amount of compact snow, followed by a fast melting in June, when in about two weeks the TG-NM counting rate returns normal.

The blue points reported in the same figure represent the total volume of snow water equivalent (SWE) in the Aosta Valley region, evaluated by the Regional Environmental Protection Agency [ARPA website] in five winter seasons, taking into account many measurements made in different locations. Note the high peak in spring 2020, where also the TG-NM suffered a larger absorption.

3.2. Rem counters dose rates

The average neutron H*(10) dose rate measured by the rem counters in different periods from 2014 to 2019 are reported in Table 1 (column 5). For completeness the Table also reports older measurement made with ALNOR, Studsvik and LINUS rem counters when the Neutron Monitor was not yet installed.

The data of rem counters working in the same energy ranges are in reasonable agreement, taking into account the large systematics errors (about 20%) of this type of instruments, and also considering that the measurements have been made in periods with different solar activity

and atmospheric conditions. The "standard" rem counters measured H* (10) values between 35 ± 2 and 54 ± 2 nSv/h, while the "extended range" ones between 76 ± 4 and 97 ± 10 nSv/h.

It is interesting to compare these data with the ambient dose equivalent rates obtained using the analytical formulation of the neutron spectrum (based on the results of simulations) developed by [Sato and Niita, 2006], given as a function of four parameters: 1) the altitude above the sea level, 2) the vertical rigidity cutoff, 3) the solar modulation potential, 4) the content of water in the ground (in terms of mass fraction w). The accuracy of the analytical functions was verified by the authors by comparing their calculations with experimental measurements made in Japan at different altitudes by [Kowatari et al., 2005].

The solar modulation potentials (reported in Table 1, column 4) are taken from a monthly database [Oulu University website] reconstructed from the ground based cosmic ray data, using the procedure by [Usoskin et al., 2017] and using the Local Interstellar spectrum (LIS) given by [Vos and Potgieter, 2015].

The content of water in the ground is crucial for the dose assessment, since the hydrogen contained in water is very efficient in thermalizing neutrons. Since it is difficult to assess in a realistic way the water fraction in the ground, we calculate the neutron spectra for two values that could reasonably be assumed as the minimum and maximum values for the Testa Grigia environment: $w = 0.2$ and $w = 0.8$. Fig. 5 shows the spectra obtained by the Sato and Niita formulations for some values of w. From

Table 1

H*(10) dose rate measured by different detectors at the Testa Grigia Laboratory. The first five rows report the data of "standard" rem counters, the following two rows report the data of "extended range" rem counters. The last rows refer to the data of the Liulin–AR spectrometer, where H*(10) has been evaluated according two different methods (see text). The errors of the measured dose rates represent the standard deviation of daily average doses. The dose rate measurements are compared with the theoretical values obtained using the [Sato and Niita, 2006] formulation for the neutron spectrum, given in the last column. The theoretical dose rates are given for two different values of the water fraction in the ground, $w = 0.8$ and $w = 0.2$ (see text).

| Instrument	Neutron energy range	Time	Solar modulation potential (GV)	H*(10) average measured dose rate (nSv/h)	H*(10) theoretical dose rate (nSv/h)
Rem counter ALNOR	thermal– 17 MeV	1996 June/July	506	47 ± 5	52–71
Rem counter Studsvik	thermal – 17 MeV	1996 June/July	506	42 ± 3	52–71
Rem counter Atomtex BDKN-03	thermal – 14 MeV	2014 November	648	49 ± 2	48–66
Rem counter Atomtex BDKN-03	thermal – 14 MeV	2017 September	522	54 ± 2	49–68
Rem counter KWD Digipig	thermal – 17 MeV	2018 November/2019 April	430	35 ± 2	53–72
–	–	–	–	–	–
Extended rem count. LINUS	thermal – 0.4 GeV	1996 June/July	506	97 ± 10	97–119
Extended rem count. Wendi-2	thermal – 5 GeV	2014 November	648	76 ± 4	100–121
–	–	–	–	–	–
Liulin-AR Total dose	–	2019 Feb./Apr.	427	240–340	–
Liulin-AR High-LET dose	–	2019 Feb./Apr.	427	86–118	104–126
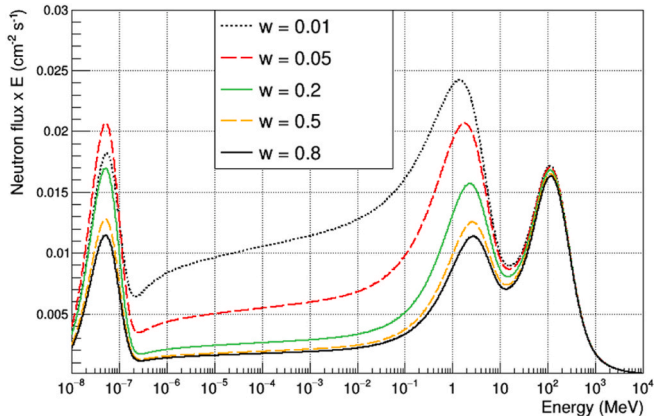
Fig. 5. Neutron spectrum at the Testa Grigia site according to the analytical formulation by [Sato and Niita, 2006] for five different values of the water fraction in the ground (w). The modulation potential is set to 300 GV.

the figure one can see that the water content affects the neutron flux up to energies of ~20 MeV. At higher energy the flux is practically unchanged.

From the neutron spectra, the expected ambient dose equivalent rates H*(10) are calculated folding the spectrum with the fluence-to-dose conversion coefficients of ICRP Publication 74 [1997] given for energies up to 1 GeV, and extended up to 10^4 GeV by the [Pelliccioni, 2000] evaluations. It has to be noted that the International Commission on Radiological Protection (ICRP) has revised the quality factors for neutrons [ICRP Publication 103, 2007], modifying the conversion curve between the neutron fluence and the *effective* dose [ICRP Publication 116, 2010]. However, according to the Commission, the ambient dose equivalent H*(10) continues to provide a good approximation for the effective dose in the energy range considered in ICRP Publication 74.

Table 1 (column 6) reports the obtained expected dose rates in the sensitive energy range of each detector (column 2). For these values, one can see that the dose due to neutrons of energy less than 14–17 MeV, i.e. without cascade neutrons, is about half of the total dose.

Comparing the measured dose rates with calculations, it is evident

that most experimental values are lower than theoretical ones, also in summer, even below the value correspondent to the water fraction $w = 0.8$. However, the Sato and Niita evaluations can only give an approximate indication of the real neutron dose, since they do not take into account the topography of the site, and the possible moderation and absorption effects of materials around the detector. In their model the experimental site has a very simple configuration, consisting of a flat and uniform ground, with fixed elemental composition and water fraction, over which the detector is located, at 2 m above the soil.

In our case, several features can significantly alter the theoretical neutron spectrum. First of all, the presence of a thick and high concrete wall of the cableway building (built in 1991) very close to the laboratory causes a significant absorption and moderation of neutrons arriving from the North direction. On the laboratory roof, the metal platform previously described with several instrumental devices on it contributes to the absorption as well. The laboratory is located on the edge of a vertical cliff. The presence of a precipice just outside of the laboratory affects the flux of albedo neutrons produced in the ground. On the opposite side, at a distance of ~50 m, there is an almost flat glacier with snow/ice all around the year. During winter and spring time an additional layer of snow covers the glacier and the rocks over which the laboratory is built and strong winds accumulate big amounts of snow against the walls of the laboratory.

An accurate simulation of the secondary neutron flux and its interactions with ice, rocks, buildings, and other artifacts surrounding the detector would be necessary to assess the absolute value of the neutron flux hitting the detector, but this is beyond the scope of this paper.

Spectrum measurements by [Mares et al., 2020] made in September 2018 with a Bonner Sphere Systems in two different positions at Jungfraujoch (Sphinx cupola at 3580 m and Research Station at 3475 m) show how the topography of the site affects the neutron spectral shape. A strong reduction of the evaporation peak and an increase of the thermal peak are observed in the data taken at the Research Station (RS), located on a steep rocky slope, with respect to those taken on the rocky summit where the Sphinx cupola is built, due to the moderation effect of the rocky slope, and partially of the RS roof. No snow was present near the two locations at the time of measurement. The corresponding H*(10) dose rate deduced from the spectrum for the Sphinx cupola was 182 nSv/h, while at the RS position was 110 nSv/h. This big difference is not

explained by the small different altitude (105 m) of the sites.

The Sato and Niita formulation (setting $w = 0.2$) gives $H^*(10) = 144$ nSv/h for the Sphinx Cupola and $H^*(10) = 133$ nSv/h for the Research Station. Since dose rate absolute values can be affected by systematics, both in measurements and in calculations, we consider the ratio between dose rates, that should be a more reliable value. According to calculations, the ratio between the dose rate in the Sphinx cupola and in the RS is 1.08, as expected by the difference in altitude, while the experimental ratio is 1.65, demonstrating that a very large fraction of neutron dose can depend on the environment topography.

3.3. Liulin-AR dose rate

We collected data with the Liulin spectrometer for 74 days in spring 2019.

For each particle giving a signal in the silicon diode, the Liulin spectrometer measures the deposited energy. Every fixed time interval (5 min in this measurement) the acquisition program writes on disk the corresponding 256-channel spectrum. Summing the deposited energy over the ADC channels, one obtains the absorbed dose in silicon:

$$D_{Si} = \frac{1}{m} \sum_{i=1}^{256} N_i \varepsilon_i \qquad (1)$$

where N_i is the number of events corresponding to the ith ADC channel, ε_i is the energy corresponding to the ith ADC channel and $m = 1.398 \ 10^{-4}$ kg is the mass of the silicon diode.

In the 74 days in which the Liulin-AR has been operating at Testa Grigia, the average counting rate was 0.158 Hz and the average absorbed dose in silicon was $D_{Si} = 171 \pm 7$ nGy/h (the error represents the standard deviations of the daily dose).

According to [Dachev, 2009], the signals with a deposited energy less than ~1 MeV corresponds to low Linear Energy Transfer (LET) events, due to ionizing particles as muons or electrons-positrons crossing the detector or to gamma ray interactions. On the contrary, the signal with deposited energy above ~1 MeV corresponds to high LET events, that at ground level are mostly due to neutron interactions. Defining low-LET events the signals with deposited energy less than 1 MeV and high-LET events the signals with deposited energy larger than 1 MeV, the average low-LET counting rate is 0.155 Hz, corresponding to an absorbed dose rate of 150 nGy/h, while the average high-LET counting rate is 0.0025 Hz, corresponding to an absorbed dose rate of 21 nGy/h.

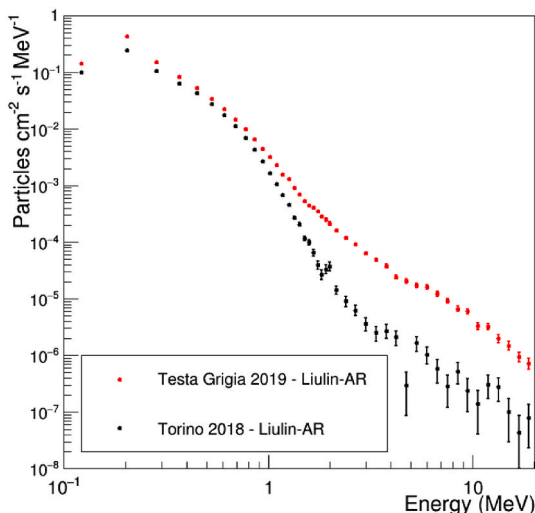Fig. 6 shows the deposited energy spectrum obtained by the Liulin-

Fig. 6. Spectrum of deposited energy in silicon measured by the Liulin-AR spectrometer at the Testa Grigia Laboratory in 2019 and at the Torino Physics Department in 2018.

AR at the Testa Grigia Laboratory. Channels above 2 MeV have been combined to reduce the statistical error. A spectral hardening above ~1–2 MeV is evident, due to the neutron component. As a comparison, the spectrum obtained in spring 2018 at the Physics Department in Torino (45.07° N, 7.69° E, 239 m a.s.l., $R_V = 4.97$ GV in 2015) in 68 days of measurement is also reported. Above ~2 MeV the two spectra differ by a factor ~10, as expected by the different site altitudes (the slightly higher rigidity in Torino has an almost negligible influence on the neutron spectrum).

The Liulin spectrometer provides the absorbed dose in silicon, but it is possible to evaluate, in an approximate way, the ambient dose equivalent $H^*(10)$.

According to [Ploc et al., 2010], $H^*(10) = a \ D_{low} + b \ D_{high}$, where D_{low} is the absorbed dose rate with deposited energy $E_d < 1$ MeV and D_{high} the absorbed dose rate with $E_d > 1$ MeV. The coefficients a and b are specific weights that have been determined experimentally and are given in the cited paper as a function of the ratio $R_D = D_{low}/D_{high}$. With this procedure, the average value of $H^*(10)$ at Testa Grigia is 340 nSv/h, while the high-LET $H^*(10)$ component is 118 nSv/h. This procedure cannot be applied to low altitude data (for example Torino data) because the neutron flux decreases significantly with respect to the low-LET component and R_D becomes too large to be used in the Ploc et al. formulation.

An alternative procedure to evaluate $H^*(10)$ by the Liulin designer T. Dachev (personal communication) gives $H^*(10) = D'_{low} + 5 \ D'_{high}$, where D'_{low} is the absorbed dose rate with $E_d < 1.16$ MeV and D'_{High} is the absorbed dose rate above this energy. In this way we obtain the total dose rate $H^*(10) = 240$ nSv/h and a high-LET dose rate $H^*(10) = 86$ nSv/h, more consistent with the extended rem counter data than the previous procedure. Using the same method for Torino data we obtain a total dose rate $H^*(10) = 117$ nSv/h and a high-LET dose rate $H^*(10) = 12.3$ nSv/h, consistent with the Saato and Niita formulation that gives $H^*(10) = 11.4$ nSv/h (setting $w = 0.2$).

3.4. Dose rate variations

To study the dose variations it is useful to compare the rem counter data with the neutron monitor counting rates in the periods when the instruments were simultaneously operating. This allows to disentangle the variations due to solar activity modulations, air pressure and local phenomena as the snow absorption effect. The comparison of TG-NM and JF-NM data allow us to evaluate the snow absorption effect on TG-NM counting rates.

In this section we report some measurements made in two periods with different solar activity: in 2014 near the maximum of 24th solar cycle and in 2018/2019 near the minimum.

In 2014, from November 14 to December 8, data have been collected for 25 days with the BDKN-03 and Wendi-2 rem counters. As for the neutron monitor counting rates, the variations of the dose rates are mainly due to the combination of atmospheric pressure, solar modulation and snow absorption. Comparing the TG-NM data (pressure corrected) with those of JF-NM we deduced that in these days there was an almost constant level of neutron absorption by the snow, varying between 6.5% and 7.7%. On the contrary, the solar modulation was much larger, being that period close to the solar maximum.

Fig. 7 shows the percent variations of the two neutron monitors counting rates every 2 h. The pressure corrected data show both a variation of about ±5% with respect to the mean value, as a response to the influence of the different interplanetary structures sweeping the Earth in that period.

The 24 h anisotropy is visible as a daily oscillation of amplitude of order ±1%. The TG-NM pressure corrected counts show a modulation very similar to that of JF-NM, due to the solar activity, since the snow effect is almost constant in the measurement period. The uncorrected data of the Testa Grigia NM shows large abrupt fluctuations due to the combination of atmospheric pressure variation and solar modulations.
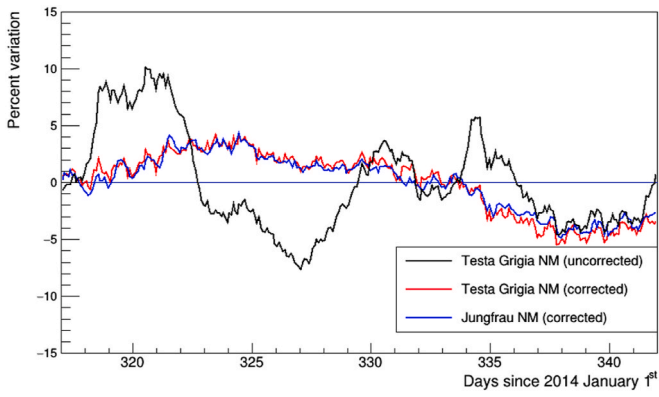
Fig. 7. Percent variation of the TG neutron monitor counting rates (uncorrected and corrected for the pressure) as a function of time, compared with the Jungfraujoch data (pressure corrected), from November 14 to December 8, 2014.

It is interesting to study the behavior of rem counters in the same period. Fig. 8 shows the daily percent variations of the BDKN-03 and Wendi-2 rem counters, compared to the variations of the neutron monitor counting rate (pressure uncorrected). The dose variations follow quite well the neutron monitor trend, in particular the dose measured by Wendi-2. Assuming a linear correlation between the counting rates of the different instruments, to quantify the correlation we determined the parameters k and D_0 of the function $D = k\,C + D_0$ that best fits the data, where D and C are the daily percent variations (with respect to the corresponding mean values) of the dose rate and the TG-NM counting rate, respectively. The best fit parameters are given in Table 2, together with the Pearson correlation coefficient R that measures the strength of the correlation. The parameter D_0 has been found consistent with zero for both instruments, as expected. The values $R = 0.82$ and $k = 1.05 \pm 0.16$ for the Wendi-2 indicate that the percent variations of this rem counter and the neutron monitor rates have similar amplitudes, while the BDKN-03 with $R = 0.64$ and $k = 0.58 \pm 0.14$ is clearly less "reactive" to the causes of NM counts variations. This is not surprising since the Wendi-2 detects neutrons with energies up to 5 GeV, a range that overlaps the neutron monitor energy range. The BDKN-03 on the contrary is mainly sensitive to neutrons of energy below 14 MeV, whose flux is more influenced by local conditions [Rühm et al., 2012; Hubert et al., 2016; Mares et al., 2020].

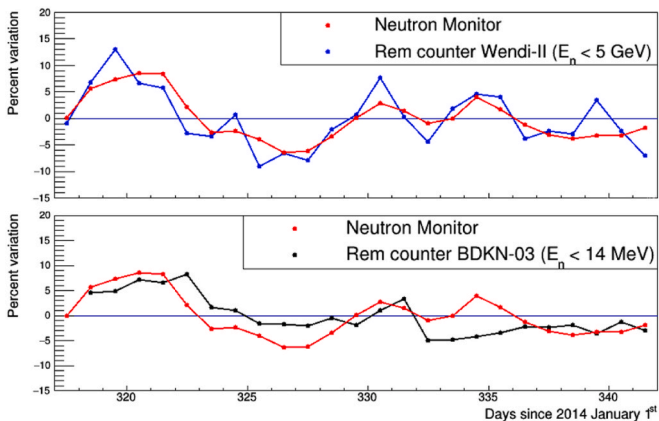In winter-spring 2018/2019 an other dosimetric monitoring has

Fig. 8. Daily percent variation of the neutron ambient dose equivalent measured by the Wendi-2 and Atomtex BDKN-03 rem counters as a function of time, compared to the Testa Grigia Neutron Monitor counting rate percent variations (uncorrected for pressure). The points represent the daily average, from November 14 to December 8, 2014.

Table 2

Best fit values of the parameters describing the correlation of the dose rate measured by different detectors with the neutron monitor counting rates (see text). R is the Pearson correlation coefficient.

	k	D_0	R
R.C. Wendi-2	1.05 ± 0.16	0.10 ± 0.65	0.82
R.C. BDKN-03	0.58 ± 0.14	0.03 ± 0.61	0.64
R.C. Digipig	0.83 ± 0.08	0.004 ± 0.46	0.70
Liulin low-LET	0.39 ± 0.03	0.001 ± 0.14	0.89
Liulin high-LET	1.50 ± 0.22	0.003 ± 1.17	0.66

been performed with different instruments: a Digipig rem counter (sensitive up to 17 MeV) and a Liulin spectrometer. The upper panel of Fig. 8 shows the percent variations (averaged over 3 days) of the TG-NM counting rate and Digipig dose rate during 210 days of measurement, together with the counting rate variations of the Liulin spectrometer during 66 days. In the 210 days period the JF-NM counting rate shows variations of amplitude less than 2% due to the very low solar activity. The snow absorption effect on the TG-NM data ranges between 5% and 13%, as shown in the lower panel of the same figure. For the Digipig and Liulin we performed the same correlation analysis described before, obtaining the best fit parameters given in Table 2. Also in this case we found the value of D_0 consistent with zero.

The correlation study between the Digipig dose rates and the TG-NM counting rates, gives $R = 0.70$ and $k = 0.83 \pm 0.08$, indicating a better response of Digipig to high energy neutrons with respect of BDKN-03.

Fig. 10 shows in more detail the daily variations in the period in which the Digipig, the Liulin and TG-NM worked simultaneously. The Liulin dose rates shows a significant correlation with the neutron monitor data. We study the Liulin correlation with the neutron monitor data separating the low-LET dose and the high-LET dose (deposited energy $E_d < 1$ MeV and $E_d > 1$ MeV respectively). The low-LET dose is well correlated with the neutron monitor counts (Pearson coefficient $R = 0.89$) but with a low value of $k = 0.39 \pm 0.03$, due to the fact that the Liulin low-LET dose is not due to neutrons (see discussion in 3.5). The high-LET dose has a worst correlation because of the low statistics, but the value of $k = 1.50 \pm 0.22$ is consistent with the idea that the high-LET signals are due to neutron interactions.

3.5. Barometric coefficient

The atmospheric pressure is one of the main causes of dose rate variations. To study the effect of the pressure, it is necessary to select a time interval when the variations of different origin are much smaller than the atmospheric effect.

The lower panel of Fig. 9 shows that in the period from Nov 27, 2018 (day 330) to May 11, 2019 (day 460) the solar modulations, derived from the pressure-corrected JF-NM data, did not exceed ±2%, and the snow absorption effect of the NM-TG counting rates was almost stable, varying between 5% and 8%. Given the small variations due to solar modulation and snow absorption, this period is suitable to study the dependence of the Digipig and Liulin data from the atmospheric pressure.

The cascade neutrons flux φ is related to the atmospheric pressure p by the expression [Bütikofer, 2018]:

$$\varphi(p) = \varphi(p_0)e^{-\beta\,(p-p_0)} \tag{2}$$

where p_0 is a reference pressure value. The barometric coefficient $\beta = 1/\lambda_{abs}$ is the inverse of the attenuation length of the neutron component in the atmosphere λ_{abs} (given in hPa). For neutron monitors, β has typical values around 0.7–0.8% hPa^{-1}, depending on the detector location. We use a similar exponential function to describe the pressure dependence of rem counters and Liulin counting rates. Then we determine the corresponding barometric coefficients by a fitting procedure.

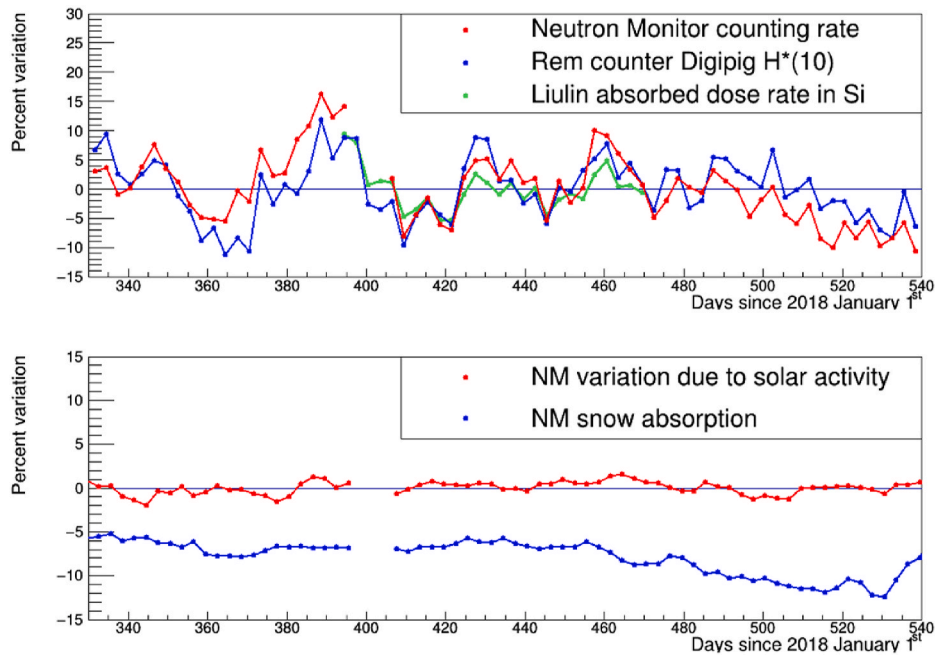Fig. 11 shows the daily percent variations of the Digipig and Liulin

Fig. 9. Upper panel: percent variations of the neutron monitor counting rate (uncorrected for pressure) and the Digipig dose rate in winter and spring 2018/2019, averaged over 3 days. Lower panel: blue points represent the decrease of the TG-NM pressure corrected counting rate due to snow absorption, red points represent the percent variations due to solar modulation given by the Jungfraujoch NM data.
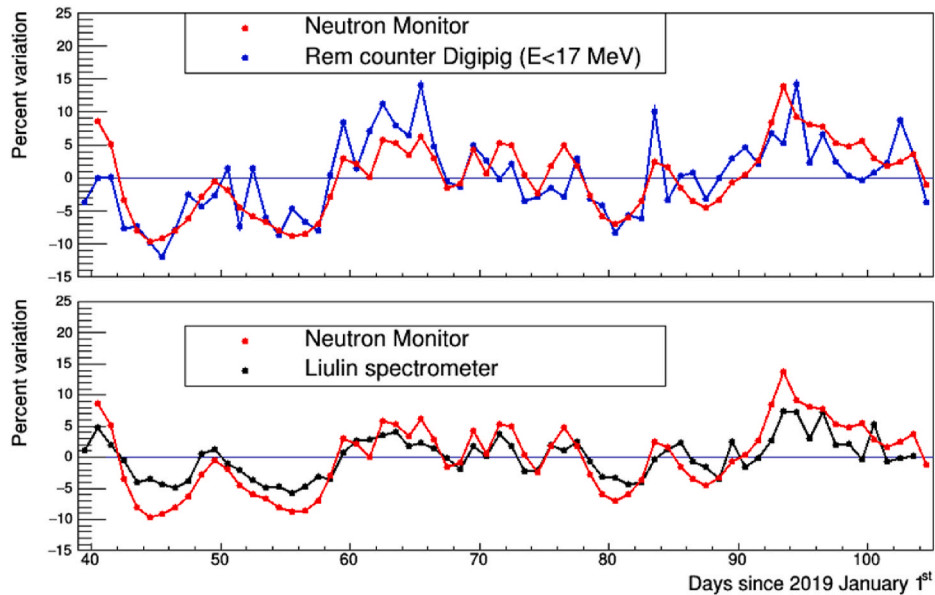

Fig. 10. Daily percent dose rate variation measured by the rem counter Digipig (upper panel) and the Liulin-AR spectrometer (lower panel), compared to the neutron monitor counting rate percent variations (uncorrected for pressure). The points represent the daily average from February 9 to April 15, 2019.

data as a function of pressure variations. The Liulin low-LET dose rate and high-LET dose rate have been considered separately. The straight lines represent the best fit to the data using the function:

$$\frac{(D - D_m)}{D_m} \, 100 = \alpha + \beta(p - p_m) \qquad (3)$$

where D_m is the average dose rate and p_m the average pressure. The parameters α and β have been determined by the fitting procedure and their values are reported in Table 3.

The Digipig data show a significant anti-correlation with pressure with a barometric coefficient $\beta = -0.56 \pm 0.06\%$ hPa^{-1}, smaller than

that of the neutron monitor ($\beta = 0.72\%$ hPa^{-1}). A smaller coefficient can be qualitatively understood considering that a low pressure is in general associated to a higher humidity in air and ground, that makes the moderation process more efficient. For this, the increase of the dose due to a lower pressure can be diminished by the moderation effect that reduces the flux of evaporation neutrons. In fact, the spread of the points around the best fit line is larger than what expected by pure statistical fluctuations (expected to be around 3.4%), indicating the existence of additional sources of variation beside air pressure.

The Liulin dose rates have different barometric coefficients for low-LET data and high-LET data, confirming the different nature of particles that mainly contribute to the two different ranges of energy deposition.
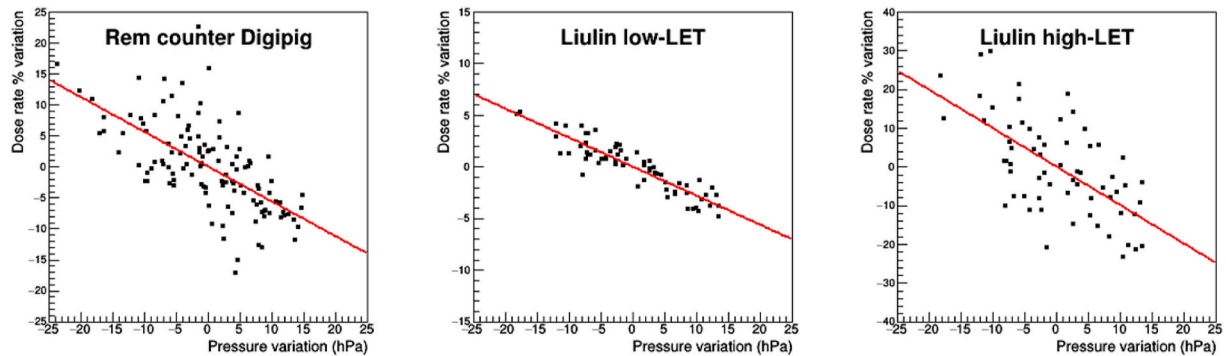
8

Fig. 11. Daily percent variation of the counting rate of different detectors at the Testa Grigia laboratory as a function of the atmospheric pressure variations.

Table 3
Coefficients of the function describing the dependence of the Digipig and the Liulin dose rates on the atmospheric pressure (see text). β is the barometric coefficient.

	β (% hPa^{-1})	α
R.C. Digipig	-0.56 ± 0.06	0.0032 ± 0.49
Liulin low-LET	-0.28 ± 0.02	0.0006 ± 0.13
Liulin high-LET	-0.99 ± 0.15	0.0023 ± 1.19

For low-LET data we obtained β = − 0.28 ± 0.02% hPa^{-1}, a value significantly smaller than the neutron monitor coefficient. Liulin low-LET counts are mostly due to ionizing charged secondary cosmic rays (mostly electrons-positrons and muons) and electrons and gamma rays from the local radioactivity due to radioelements in the rocks under the laboratory. The barometric coefficient of charged particles of air showers is ⌣1% hPa^{-1} but the contribution of the radioactivity (that we have not evaluated) is pressure independent and can reduce significantly the pressure effect on the total counting rate [Aielli et al., 2008]. The Liulin barometric coefficient that we found is consistent with the value β = −0.34 ± 0.03% hPa^{-1} obtained by [Kubancak et al., 2014], with a Liulin spectrometer at the Jungfraujoch station.

The barometric coefficient for the Liulin high-LET dose is β = − 0.99 ± 0.15% hPa^{-1}. The large spread of the points around the best fit curve are mainly due to statistical fluctuations (the average counting rate is 216 day^{-1} hence the standard deviation of daily fluctuations is 7%). The value of the barometric coefficient is higher than that of the neutron monitor (but not really inconsistent), but more statistic is necessary to assess its value with more accuracy.

4. Conclusions

In the present study we reported the results of neutron dosimetric measurements performed during the last years at the Testa Grigia Laboratory with various instruments, with the aim of studying the dose rate variations under different solar activity and environmental conditions and to test the response of the instruments to the neutron flux changes.

The installation of a neutron monitor in the laboratory in 2014 allows to assess the variations of the cosmic ray neutron flux with high accuracy and is of great help to disentangle the different sources of dose variations. The comparison of the pressure-corrected data of the neutron monitor installed in the laboratory with the public data of the 18-IGY neutron monitor located at Jungfraujoch at similar altitude and rigidity cutoff, allows us to evaluate the local effects (besides atmospheric pressure variations) that could alter the dose measurement, as the accumulation of snow on the roof of the laboratory, that in winter can be significant.

In November 2014, near solar maximum, we performed dosimetric measurements made with two different rem counters, an Atomtex BDKN-03 and an "extended range" Thermo Wendi-2. In winter 2018/

2019, a period near solar minimum, we performed measurements with a rem counter KWD Digipig and a Liulin-MDU spectrometer, that measures the energy deposited in a silicon diode.

These instruments (except the Digipig rem counter) have been used in Antarctica during the dosimetric campaigns CORA [Zanini et al., 2015] and HALCORD in several periods from 2014 to 2020 [Zanini et al., 2019].

All instruments showed an evident correlation with the TG neutron monitor pressure uncorrected data. In particular, percent variations of Wendi-2 dose rates and neutron monitor counting rates were consistent with each other, as one expects due to the overlapping of their energy range.

Selecting a sub-period when the effect of the snow on TG-NM counts was constant, it was possible to study the dependence of the dose measured by the Digipig and the Liulin on the atmospheric pressure, and to evaluate the correspondent barometric coefficients.

To quantify the effects of the environment on the neutron doses, we are developing a complete simulation of the air shower particles in atmosphere taking into account the site topography, the geometry of materials over and around the detector as the hut roof and other structures near the laboratory, and also considering the presence of snow accumulations in particular places.

On the other hand, from the experimental point of view, the measurement of the neutron dose will be carried on in the next years continuously and with dedicated instruments, monitoring the dose along the ascending phase of the 25th solar cycle, that started in 2020. The data will be a term of comparison for the two dosimetric campaigns planned for 2022–2023 in the southern hemisphere, in the Antarctica base Concordia (project CORDIAL of the Italian National Antarctic Research Program, PNRA) and in the South Atlantic Magnetic Anomaly region (project SAMADHA of the National Institute of Nuclear Physics, INFN [samadha website]).

CRediT authorship contribution statement

S. Vernetto: Investigation, Software, Writing – original draft, Writing – review & editing. **M. Laurenza:** Investigation. **M. Storini:** Investigation. **A. Zanini:** Funding acquisition, Supervision. **P. Diego:** Investigation. **S. Massetti:** Software. **A. Liberatore:** Data curation. **J.C. Terrazas:** Data curation. **C. Vigorito:** Software, Data curation. **P. Vallania:** Data curation. **S. Cirilli:** Data curation.

Declaration of competing interest

The authors declare that they have no known competing financial interests or personal relationships that could have appeared to influence the work reported in this paper.

References

Aielli, G., et al., ARGO-YBJ Collaboration, 2008. Scaler mode technique for the ARGO-YBJ detector. Astropart. Phys. 30, 85–95. https://doi:10.1016/j.astropartphys.2008.07.002.

Bütikofer, R., 2018. Ground-based measurements of energetic particles by neutron monitors. In: Malandraki, O., Crosby, N. (Eds.), Solar Particle Radiation Storms Forecasting and Analysis, Astrophysics and Space Science Library, vol. 444. Springer, Cham. https://doi.org/10.1007/978-3-319-60051-2_6.

Cheminet, A., Hubert, G., Lacoste, V., Boscher, D., 2014. Measurements and Monte Carlo simulations of the spectral variations of the cosmic-ray-induced neutrons at the Pic du Midi over a 2-y period. Radiat. Protect. Dosim. 161 (4), 284–289. https://doi.org/10.1093/rpd/nct330.

Clem, J.M., Dorman, L.I., 2000. Neutron monitor response functions. Space Sci. Rev. 93 (1–2), 335–359. https://doi.org/10.1023/A:1026508915269.

Dachev, T.P., 2009. Characterization of the near Earth radiation environment by Liulin type spectrometers. Adv. Space Res. 44, 1441–1449. https://doi.org/10.1016/j.asr.2009.08.007.

Flückiger, E.O., Bütikofer, R., 2009. Swiss neutron monitors and cosmic ray research at Jungfraujoch. Adv. Space Res. 44, 1155–1159. https://doi.org/10.1016/j.asr.2008.10.043.

Hess, W.N., Patterson, H.W., Wallace, R., 1959. Cosmic-ray neutron energy spectrum. PRD 116, 2.

Hubert, G., Panzianotto, M.T., Federico, C.A., 2016. Modeling of ground albedo neutrons to investigate seasonal cosmic ray-induced neutron variations measured at high altitude stations. J. Geophys. Res. Space 121, 12186–12201. https://doi.org/10.1002/2015JA021654.

ICRP (International Commission on Radiological Protection), 1997. Conversion Coefficients for Use in Radiological Protection against External Radiation, vol. 74. Pergamon Press, Oxford. Publication.

ICRP (International Commission on Radiological Protection), 2007. The 2007 Recommendations of the International Commission on Radiological Protection, vol. 103. Publication.

ICRP (International Commission on Radiological Protection), 2010. Conversion coefficients for radiological protection quantities for external radiation exposures, publication 116. Ann. ICRP 40 (2–5).

Kowatari, M., Nagaoka, K., Satoh, S., Ohta, Y., Abukawa, J., Tachimori, S., Nakamura, T., 2005. Evaluation of the altitude variation of the cosmic-ray induced environmental neutrons in the Mt. Fuji area. J. Nucl. Sci. Technol. 42, 495–502. https://doi.org/10.1080/18811248.2004.9726416.

Kubancak, J., Ambrozova, I., Bütikofer, R., Kudela, K., Langer, R., Davidkova, M., Ploc, O., Malusek, A., 2014. Liulin silicon semiconductor spectrometers as cosmic ray monitors at the high mountain observatories Jungfraujoch and Lomnický štít. J. Instrum. 9, P07018 https://doi.org/10.1088/1748-0221/9/07/P07018.

Manfredotti, C., Ongaro, C., Zanini, A., Cavaioli, M., Tommasino, L., 1997. Spectrometry of low and high energy neutrons by unfolding passive detector responses. Proc. Int. Conf. Neutrons Res. Industr. 2867.

Mares, V., Brall, T., Bütikofer, R., Rühm, W., 2020. Influence of environmental parameters on secondary cosmic ray neutrons at high-altitude research stations at Jungfraujoch, Switzerland, and Zugspitze, Germany. Radiat. Phys. Chem. 168, 108557 https://doi.org/10.1016/j.radphyschem.2019.108557.

Moraal, H., Belov, A., Clem, J., 2000. Design and co-ordination of multi-station International neutron monitor networks. Space Sci. Rev. 93, 285–303. https://doi.org/10.1023/A:1026504814360.

Nakamura, T., Nunomiya, T., Abe, S., Terunuma, K., Suzuki, H., 2005. Sequential measurements of cosmic ray neutron spectrum and dose rate at sea level in Sendai, Japan. J. Nucl. Sci. Technol. 42, 843. https://doi.org/10.1080/18811248.2005.9711035.

Pelliccioni, M., 2000. Overview of the fluence-to-effective dose and fluence-to-ambient dose equivalent conversion coefficient for high energy radiation calculated using the FLUKA code. Radiat. Protect. Dosim. 88 (4), 01448420 https://doi.org/10.1093/oxfordjournals.rpd.a033046, 279.

Ploc, O., Brabcová, K., Spurný, F., Dachev, T., 2010. Use of energy deposition spectrometric Liulin for individual monitoring of aircrew. Radiat. Protect. Dosim. 144, 1–4. https://doi.org/10.1093/rpd/ncq505.

Rühm, W., Ackermann, U., Pioch, C., Mares, V., 2012. Spectral neutron flux oscillations of cosmic radiation on the Earth's surface. J. Geophys. Res. 117, A08309 https://doi.org/10.1029/2012JA017524.

Rühm, W., Mares, V., Pioch, C., Simmer, G., Weitzenegger, E., 2009. Continuous measurements of secondary neutrons from cosmic radiation at mountain altitude and close to the North Pole – a discussion in terms of H*(10). Radiat. Protect. Dosim. 136 (4), 256–261. https://doi.org/10.1093/rpd/ncp161.

Sato, T., Niita, K., 2006. Analytical functions to predict cosmic-ray neutron spectra in the atmosphere. Radiat. Res. 166, 544–555. https://doi.org/10.1667/rr0610.1.

Signoretti, F., Storini, M., 2011. A new modular cosmic-ray detector. Astrophys. Space Sci. Trans. 7, 11–14. https://doi.org/10.5194/astra-7-11-2011.

Signoretti, F., Storini, M., Marcucci, M.F., Laurenza, M., 2013. Performance test of a large modular cosmic-ray detector. J. Phys. Conf. 409 (1) article id. 012045.

Usoskin, I.G., Gil, A., Kovaltsov, G.A., Mishev, A., Mikhailov, V.V., 2017. Heliospheric modulation of cosmic rays during the neutron monitor era: calibration using PAMELA data for 2006-2010. J. Geophys. Res. Space Phys. 122, 3875–3887. https://doi.org/10.1002/2016JA023819.

Vega-Carrillo, H.R., Manzanares-Acuna, E., 2004. Background neutron spectrum at 2420 m above sea level. Nucl. Instrum. Methods A 524, 146–151. https://doi.org/10.1016/j.nima.2004.01.044.

Vos, E.E., Potgieter, M.S., 2015. New modeling of galactic proton modulation during the minimum of solar cycle 23/24. Astrophys. J. 815, 119. https://doi.org/10.1088/0004-637X/815/2/119.

Zanini, A., Ongaro, C., Manfredotti, C., Tommasino, L., Miranda Losa, P., 2001. Neutron spectrometry at various altitudes in atmosphere by passive detector technique. Il Nuovo Cimento 24C (4–5), 691–697. https://doi.org/10.1016/j.jastp.2005.01.005.

Zanini, A., Storini, M., Visca, L., Durisi, E., Fasolo, F., Perosino, M., Borla, O., Saavedra, O., 2005. Neutron spectrometry at high mountain observatories. J. Atmos. Sol. Terr. Phys. 67, 755. https://doi.org/10.1016/j.jastp.2005.01.005.

Zanini, A., Storini, M., Saavedra, O., 2009. Cosmic rays at high mountain observatories. Adv. Space Res. 44, 1160. https://doi.org/10.1016/j.asr.2008.01.039.

Zanini, A., Ciancio, V., Laurenza, M., Storini, M., Esposito, A., Terrazas, J.C., Morfino, P., Liberatore, A., Di Giovan, G., 2015. Environmental radiation dosimetry at Argentine Antarctic Marambio Base (64°13′ S, 56°43′ W): preliminary results. J. Environ. Radioact. 175–176, 149–157. https://doi.org/10.1016/j.jenvrad.2017.04.011.

Zanini, A., Vernetto, S., Ciancio, V., Di Giovan, G., Morfino, P., Liberatore, A., Giannini, G., Hubert, G., 2019. Environmental radiation dosimetry at high southern latitudes with Liulin type instruments. J. Environ. Radioact. 208–209, 105993 https://doi.org/10.1016/j.jenvrad.2019.105993.

Zweck, C., Zreda, M., Desilets, D., 2013. Snow shielding factors for cosmogenic nuclide dating inferred from Monte Carlo neutron transport simulations. Earth Planet Sci. Lett. 379, 64–71. https://doi.org/10.1016/j.epsl.2013.07.023.

Websites

ARPA, Regional Environmental Protection Agency. https://www.arpa.vda.it/en/climate-change-impacts/snow/swe (accessed 24 September 2021).

LND INC., Designer And Manufacturer Of Nuclear Radiation Detector, New York, USA. http://lndinc.com/(accessed 24 September 2021).

Jungfraujoch NM data, Cosmic Rays, Physikalisches Institut, University of Bern, Switzerland. http://cosray.unibe.ch/(accessed 24 September 2021).

Meteomanz, Meteorological Data From Worldwide Locations. http://meteomanz.com (accessed 24 September 2021).

Oulu University, Cosmic Ray Station Of The University Of Oulu, Finland. https://cosmicrays.oulu.fi/phi/phi.html (accessed 24 September 2021).

SAMADHA project (South Atlantic Magnetic Anomaly Dosimetry at High Altitude), INFN, Italy. http://samadha.to.infn.it (accessed 24 January 2022).